NUMERICAL RELATIVISTIC GRAVITATIONAL COLLAPSE WITH SPATIAL TIME SLICES

Charles R. Evans
Department of Astronomy
University of Illinois
Urbana, IL 61801
and
Lawrence Livermore National Laboratory
P.O. Box 808 L-35
Livermore, CA 94550

Larry L. Smarr*
Departments of Astronomy and Physics
University of Illinois
Urbana, IL 61801

James R. Wilson
Lawrence Livermore National Laboratory
P.O. Box 808 L-35
Livermore, CA 94550

1. INTRODUCTION

In the usual flatspace hydrodynamics, there is a unique split between Eulerian and Lagrangian observers. An Eulerian observer is one at rest in space, while the Lagrangian observer is one at rest in the fluid. We can define an observer at an event in spacetime by giving his 4-velocity at that event. The path through spacetime taken by the observer is called the timeline of that observer. In flat Minkowski spacetime (the spacetime of special relativity), the Eulerian observer's 4-velocity is exceedingly simple, because the time slices (3-spaces representing a given instant of time) are parallel flat 3-planes. Since the Eulerian

*Alfred P. Sloan Fellow

K.-H. A. Winkler and M. L. Norman (eds.), Astrophysical Radiation Hydrodynamics, 491-529.
© 1986 by D. Reidel Publishing Company.

observer is at rest, his 4-velocity is normal to the time slice. He is not shearing, converging, accelerating, or rotating relative to nearby Eulerian observers. In contrast, the Lagrangian observer at the same event is doing all these things, relative to nearby Lagrangian observers. While the timelines of the Lagrangian observers, following the fluid particles, are complicated curved trajectories through spacetime, the Eulerian observer's timelines are straight and parallel to each other.

This situation changes drastically in curved spacetime, where Einstein's equations of general relativity must be solved in tandem with the hydrodynamic equations. The preferred flat time slices of Minkowski spacetime no longer exist, therefore the preferred Eulerian observers no longer exist. One must choose some smooth time slicing of spacetime, which will then define a set of Eulerian observers at rest in those time slices (Smarr, 1977; Smarr and York, 1978b). Thus, the first thing we lose is the uniqueness of the Eulerian observers. Furthermore, the resulting Eulerian observers will be shearing, converging, and accelerating in general. They will not be rotating since they are normal to the time slices. The 3-spaces that the Eulerian observers are at rest in will no longer be flat, but instead will have curvature (measured by the 3-Ricci tensor R_{ij}). The spatial partial derivatives of flatspace must be replaced by covariant derivatives with Christoffel symbols. Both the timelines of the Eulerian observers and of the Lagrangian observers are curved trajectories in the curved spacetime.

However, having accepted this conceptual generalization of the notion of Eulerian observers, Einstein's equations can be written in a form not very different from those of ordinary self-gravitating hydrodynamics. That is, there are evolution equations containing the first time derivatives of some basic variables coupled to elliptic (or parabolic) equations for some auxiliary variables. Once one has this form of Einstein's equations, one can apply standard finite-difference techniques on a spatial grid to reduce the coupled set of partial differential equations to a large set of algebraic equations.

Numerical relativity thus discretizes the spacetime continuum manifold into a spacetime lattice, the events of which are organized into a spacetime coordinate system. The unknown variables are the components of the 4-metric tensor at the lattice points. As the lattice is refined to smaller scales, the solutions converge to the continuum solution of Einstein's differential equations.

In practice, this lattice of events is built up from an initial data hypersurface by constructing a family of hypersurfaces to the future of that data. There are two fundamentally different approaches to this construction: the spacelike and the null. In

the first, the spacetime is built up from spacelike hypersurfaces starting on a Cauchy initial value surface (for a detailed definition see Eardley and Smarr, 1979). In the second, characteristic initial data is evolved using null hypersurfaces. Our paper deals with the former case using spacelike hypersurfaces. For a method which illustrates the latter case see the companion article in this volume by Stewart.

Before going into the rather complicated details of numerical relativity, we will physically motivate why such an all-out approach is necessary. Our primary objective for this code is to calculate the dynamics and emitted gravitational radiation from violent, strongfield, asymmetric, and high (internal) velocity gravitational collapse. The calculation of such energetic sources is certainly out of reach of analytic techniques. Yet it is precisely these violent events which are likely to be the most efficient sources of gravitational radiation and therefore (provided they occur frequently enough) may be the first sources detected experimentally.

Some numerical calculations, e.g. Müller (1982) and Müller and Hillebrandt (1981), have used a Newtonian hydrodynamics code with Newtonian gravity to calculate very nonspherical gravitational collapse. Then they use the standard quadrupole formula to calculate the gravitational wave form and energy loss by gravitational radiation. Their approach is to carefully treat the microphysics, but to use approximations for the gravity. Such an approach loses two major pieces of gravitational physics.

First, as the gravitational field becomes relativistic, i.e. when $\phi/c^2 \ll 1$ no longer holds, then the scalar potential ϕ representation of the gravitational field becomes invalid and the tensor representation of Einstein must be used. Another way to say this is that one must replace the gravitational acceleration $\nabla\phi$ in the hydro equations by a complicated family of potential gradients. These new terms are significant in determining the flow of the fluid in relativistic regimes. If these terms are not included, the flow calculated by a Newtonian code can begin to deviate significantly from the true flow. We call these parts of the gravitational field "longitudinal." A code which corrects this difficulty by solving the nonradiative Einstein equations is discussed by Wilson (1975).

Second, there is no useful method for calculating the gravitational radiation emitted from a relativistic problem except by calculating the full Einstein equations as we do. The use of the approximate method called the "quadrupole formula" can only be justified in nonrelativistic regimes. This formula states that the angle averaged gravitational radiation flux is given by

$$dE/dt = 0.3\ (\overset{\bullet\bullet\bullet}{I}_{zz})^2 \tag{1}$$

and the gravitational wave amplitude $h_+^{(Q)}$ is given by

$$h_+^{(Q)} = 1.5 r^{-1}\ \overset{\bullet\bullet}{I}_{zz}\ \sin^2\theta \tag{2}$$

where a raised dot denotes time derivative and units are $G = c = 1$. The quadrupole moment itself is given by

$$I_{zz} = 2\ \pi \int dr\ d\theta\ r^4\ \sin\theta\ (\cos^2\theta - 1/3)\ \rho \tag{3}$$

where the volume integral is taken over the matter density $\rho(r,\theta)$ expressed in spherical coordinates.

This quadrupole formula was derived by Landau and Lifshitz (1941) as an approximation to the Einstein equations. As Thorne (1980a, p. 289) carefully points out, the derivation breaks down if either the "slow motion" $v/c \ll 1$ or "weak field" $\phi/c^2 \ll 1$ restrictions are violated. For self-gravitating bodies where $\phi \sim v^2$, these are seen to be physically self consistent restrictions. As Thorne (1980a) points out neutron stars are therefore outside the regime of validity of the quadrupole formula.

In gravitational collapse to nuclear densities or beyond, one can get velocities of order $v/c \sim 0.2$, which violates the "slow motion" assumption. Such high velocities can cause phase shifts in the emitted radiation. This can suppress the actual amount of radiation generated, over that expected by the quadrupole moment, by destructive interference of waves. For calculations of this effect see Nakamura and Sasaki (1981) and Haugan et al. (1982).

Although the surface gravitational potential of stellar interiors at nuclear density may be "only" $\phi/c^2 \sim 0.15$, the central value can reach $\phi/c^2 \sim 0.5$, clearly violating the "weak field" condition. For such high gravitational fields, the very definition of the quadrupole moment itself, equation (3), becomes ill-defined, since the integral is not covariantly defined. The corrections which curved space makes to the lengths and time derivatives used in equation (3) are of order ϕ/c^2; their appearance as high powers in equation (1) renders the definition meaningless. For detailed examples see Evans (1984b). More intricate and sophisticated definitions of the quadrupole moment exist, which do not depend on a volume integral over strong field regions, although these still require slow motion. For a comprehensive analysis see Thorne (1980b).

In conclusion, there seems to be no "short cut" to studying the physics of relativistic core collapse. Nature is well described here only by the full theory of general relativity. The

only way known to solve the theory in the dynamic strong field regime is numerical relativity. Therefore, our approach is to calculate the gravitational physics correctly first, then later add more detailed microphysics.

The outline of our paper is as follows. In section 2 we write out the Einstein equations as they appear on a series of spacelike hypersurfaces (the "3+1" approach). We describe how the coordinate freedom (general covariance) shows up in this form of Einstein's equations. The initial value problem and the closely related problem of the constraint equations in general relativity are discussed.

Our code is discussed in section 3. It will handle any axisymmetric collapse problem as long as there is no rotation. For two different examples of how to handle rotation, see Nakamura, et al. 1980; Nakamura, 1981; and Bardeen and Piran, 1983. The particular coordinate system we use yields a set of coupled differential equations (elliptic plus hyperbolic) which we must solve for the gravitational field. Some aspects of the finite differencing of this system of partial differential equations is considered.

Finally a brief conclusion and prospectus for the future is contained in section 4.

2. DYNAMICAL APPROACH TO GENERAL RELATIVITY: GENERAL TECHNIQUES

a) Einstein equations in (3+1) formalism

The approach we will take for the Einstein equations is to evolve them as a Cauchy problem, just as one normally does for hydrodynamics. That is, one starts at t=0, in an initial data 3-space, on which one gives the starting values of the physical variables. Then one integrates forward a small amount of time using the evolution equations. This gives a sequence of initial data 3-spaces, the union of which gives the spacetime. There are only two novelties in this procedure when one is solving Einstein's equations, although both novelties are also present in Maxwell's equations of electrodynamics. The first is that the initial data for Einstein's equations are constrained, i.e. there are several elliptic type differential equations that the variables must satisfy on each time slice. The second is that one must maintain a coordinate gauge as one advances the evolution equation. In practice, this means solving some more elliptic equations on each time step.

Consider an initial data 3-space for Einstein's equations. The fundamental variable representing the gravitational field on that time slice is the 3-metric γ_{ij}. This is a symmetric 3 by 3

matrix of functions, with six independent components. Some of these functions may be identically zero in special cases. The Einstein equations yield evolution equations for those metric functions which are nonzero. Since Einstein's equations are a second order hyperbolic system, we must also have a "velocity-like" variable to be conjugate to the 3-metric which is the "position-like" variable. This turns out (Arnowitt, Deser, and Misner, 1962) to be the extrinsic curvature tensor K_{ij} which tells how the 3-space is embedded in the spacetime (Wheeler, 1963).

However, there is another interpretation (Smarr, 1975; Smarr, 1977; Smarr and York, 1978b; Smarr, Taubes, and Wilson, 1980) of K_{ij} which may appeal more to researchers in hydrodynamics. The extrinsic curvature tensor turns out just to be the negative of the expansion tensor formed from the Eulerian observer's 4-velocity. That is, if we think of the timelines of the Eulerian observers as the timelines of some imaginary fluid in the spacetime, then the trace of K_{ij} is the rate of expansion of the fluid locally, while the tracefree part of K_{ij} is the negative of the local shear tensor of the fluid. We will set our time slicing gauge by demanding that the Eulerian observer fluid be incompressible (Lichnerowicz, 1944), which will force the trace of K_{ij} to zero. The Einstein equations will then yield evolution equations for the tracefree part of K_{ij}.

We now write out formally these two evolution equations. The time derivative of the 3-metric is given by:

$$\partial_t \gamma_{ij} = \underbrace{-2\alpha\, K_{ij}}_{\text{shear}} + \underbrace{D_i\beta_j + D_j\beta_i}_{\text{convective derivatives}} \tag{4}$$

while the time derivative of K_{ij} is given by:

$$\begin{aligned}\partial_t K_{ij} = \alpha\,[&\underbrace{R_{ij}}_{\text{tides}} \underbrace{- 2\, K_{im}\, K^m_j + K^m_m\, K_{ij}}_{(\text{shear})^2}] \\ &\underbrace{- D_i D_j \alpha}_{\text{differential acceleration}} + \underbrace{\beta^m D_m K_{ij} + K_{im} D_j \beta^m + K_{mj} D_i \beta^m}_{\text{convective derivatives}} \\ &- 8\pi\alpha\,[\underbrace{S_{ij} + 1/2\, \gamma_{ij}\,(\rho_H - S^m_m)}_{\text{matter stress}}]\end{aligned} \tag{5}$$

where $c = 1$, $G = 1$. From the first equation, one can see that K_{ij} acts as a "velocity" for γ_{ij}. We will discuss the terms one by one.

The derivative operator D_i is the spatial covariant derivative. This is the same as the partial derivative on a scalar quantity, but has additional Christoffel symbols when acting on a vector:

$$D_i\beta_j = \partial_i\beta_j - \Gamma_{ij}^{k}\beta_k. \tag{6}$$

The Christoffel symbol Γ_{jk}^{i} is built out of the 3-metric by:

$$\Gamma_{ij}^{k} = 1/2\,\gamma^{km}\,(\partial_i\gamma_{mj} + \partial_j\gamma_{im} - \partial_m\gamma_{ij}), \tag{7}$$

where γ^{ij} is the matrix inverse of γ_{ij}. Thus, the Christoffel symbol is itself nonlinear in the 3-metric. Even more nonlinear is the 3-Ricci tensor in the second equation:

$$R_{ij} = \partial_m\Gamma_{ij}^{m} - \partial_j\Gamma_{im}^{m} + \Gamma_{nm}^{m}\,\Gamma_{ij}^{n} - \Gamma_{nj}^{m}\,\Gamma_{im}^{n}. \tag{8}$$

The first two terms of the Ricci tensor contain the second spatial derivatives of γ_{ij}. One can see this more clearly by rewriting (see, e.g. Smarr, 1979) the Ricci tensor as:

$$\begin{aligned} R_{ij} = {} & -1/2\;\gamma^{km}\,(\partial_i\partial_j\gamma_{km} + \partial_k\partial_m\gamma_{ij} - \partial_i\partial_m\gamma_{kj} \\ & - \partial_k\partial_j\gamma_{im}) - \gamma^{km}\gamma_{pq}\,(\Gamma_{km}^{p}\Gamma_{ij}^{q} - \Gamma_{kj}^{p}\Gamma_{im}^{q}). \end{aligned} \tag{9}$$

Therefore, if one substitutes $\partial_t\gamma_{ij}$ for K_{ij} (i.e. using eqn. (4)) in equation (5), one sees roughly that the resulting equation contains a wave operator on γ_{ij}. One of the great difficulties of numerical relativity is that in the presence on all the other terms in equations (4) and (5), the hyperbolic character of the evolution equations is much more difficult to exhibit.

In fact, the equations (4) and (5) can be rewritten in either completely second order form or in completely first order form. All three of these forms have been finite differenced and used for problems in numerical relativity (for references see Smarr, 1979). In our application using these techniques in section 3, we directly utilize the form of the equations given above.

Physically, the Ricci tensor represents the gravitational tidal stresses which cause a time rate of shear ($\partial_t K_{ij}$) in the Eulerian observers. Note that in addition to the second spatial derivative terms in Ricci, there are terms quadratic in the Christoffel symbols, which mean terms quadratic in $\partial_i\gamma_{ij}$. These have a precise analog in the next term in equation (5), which is quadratic in K_{ij}, or in $\partial_t\gamma_{ij}$. It is already clear then, that we

are going to have trouble with a time explicit finite-differencing code in getting the spatial and time derivative terms in $\partial_t K_{ij}$ centered correctly so that the balancing between the two principal nonlinear terms occurs correctly in strong field regions.

Note that the nonlinear terms in the evolution equation are of two kinds (Smarr, 1979). First, the velocity matrix in the second order wave operator on γ_{ij} depends on the 3-metric ($\sim \alpha^2 \gamma^{ij}$). Second, there are the nonlinear terms quadratic in the first space and time derivatives of the 3-metric. There is no detailed analysis of how these terms cause steepening or dispersion of wave forms in strong field regions. Furthermore, because these are tensor equations, unlike the scalar Korteweg-de Vries equation, the nonlinear terms can be reshuffled by index manipulation. For instance, it is often useful to rewrite the evolution equation (5) for $\partial_t K^i_j$ which eliminates the quadratic term $-2 K_{im} K^m_j$ in equation (5). Then on a tr(K) = 0 slice, there is no term quadratic in the time derivatives.

The matter source term in equation (5) is the material stress as seen in the rest frame of the Eulerian observers. Again, this stress causes a time rate of shear ($\partial_t K_{ij}$) in the Eulerian observers. The rest mass density ρ, the specific internal energy ε, and the pressure p of a perfect fluid are all defined in the Lagrangian rest frame of the fluid. These quantities must be Lorentz boosted to the Eulerian frame (by matter velocity V_i) to get the values of the density, momentum, and stress that are seen by the Eulerian observer. The results are (Smarr, Taubes, and Wilson, 1980):

$$\rho_H = \rho h \Gamma_2^2 - p, \quad \Gamma_2 \equiv (1 - V_i V^i)^{-1/2} \tag{10a}$$

$$S_i = -\rho h \Gamma_2^2 V_i, \quad h = 1 + \varepsilon + p/\rho \tag{10b}$$

$$S_{ij} = p\gamma_{ij} + \rho h \Gamma_2^2 V_i V_j. \tag{10c}$$

The matter terms are evolved by the general relativistic equations of hydrodynamics. We will not treat this part of the problem in this paper since it is exhaustively covered elsewhere (Wilson, 1979; Dykema, 1980; Smarr, Taubes, and Wilson, 1980; Nakamura, et al 1980; Evans, 1984a,b). The equations can be written in a form which resembles very closely the Newtonian equations of Eulerian hydrodynamics. The manner in which the transport terms [e.g. $\partial_i(AV^i)$] are differenced varies from group to group. For our approach to differencing the hydrodynamic equations see Dykema (1980). This technique is also used for treating the transport terms that appear in the reduction of equation (5) in our model (see section 3).

b) Gauge conditions

Finally, we come to the gauge terms in equations (4) and (5). The time gauge is set by the scalar lapse function α. Although two successive time slices are separated by a constant coordinate time interval Δt, the proper time separating the two slices varies over the 3-space. At any point in the 3-space the proper time interval to the next slice is $\alpha\Delta t$. Thus, the lapse function acts as a spatially variable time step, which can slow down the proper time evolution in strong field regions, thus avoiding running the time slices into the singularities inside black holes. Because the proper time step varies in space, the Eulerian observers find themselves accelerated by an amount $\partial_i \ln\alpha$, even though they remain at rest. This acceleration is required to counteract the gravitational acceleration which would otherwise make them move inward. The lapse function appears in two manners in the evolution equations (4) and (5). First, it multiplies certain terms to correct the coordinate time derivative to proper time. Second, the differential spatial acceleration $(D_i D_j \alpha)$ causes a time rate of change of the shear of the Eulerian observers.

It is often convenient to have a moving spatial coordinate system, e.g. a corotating system. This means that the timelines along which the spatial coordinates are constant do not coincide with the timelines of the Eulerian observers. At t=0 one can use any convenient spatial coordinate grid (cartesian, cylindrical, spherical, etc.) to label all points in the initial 3-surface. The coordinate timeline through a given point in the initial surface will intersect all future time slices and label one point in each time slice with the spatial coordinate that it had at t=0. In this way, the coordinate time lines provide a map which lays down a copy of the original coordinate grid on successive time slices. Just as in the case of matter discussed above, there is a local boost velocity which transforms one from the Eulerian rest frame to the coordinate rest frame. This is called the shift vector β_i. It acts in the evolution equations as a convective derivative, just as the matter velocity appears in the Euler equations of hydrodynamics.

Thus we see that the functions (α,β_i) which specify, respectively, the time and spatial coordinates are integrated directly into the partial differential evolution equations (4) and (5). However, the Einstein equations leaves one the freedom to decide which time and space coordinates are used on any given problem. That is, we must specify α and β_i on each time slice, in order to be able to evolve (γ_{ij}, K_{ij}) into the correct coordinate system.

The equation we use to specify α is the trace of equation (5):

$$\partial_t[\mathrm{tr}(K)] = \beta^i\partial_i[\mathrm{tr}(K)] - \Delta\alpha + \alpha[K_{ij}K^{ij} + 4\pi(\rho_H + S^i_i)]. \quad (11)$$

This equation gives the time rate of change of the expansion [tr(K)] of the Eulerian observers. For noncosmological spacetimes, there is no overall expansion of the physical space, so it seems natural to set the expansion equal to zero. For the cosmological case see Centrella and Wilson (1983, 1984) and Piran (1980). As remarked above, Lichnerowicz (1944) points out that setting tr(K) = 0 will make the imaginary fluid of Eulerian observers incompressible. In order to keep the trace of K_{ij} always zero, equation (11) tells us that we must solve a linear elliptic equation for α on each time slice:

$$\Delta\alpha - \alpha[K_{ij}K^{ij} + 4\pi(\rho_H + S^i{}_i)] = 0. \quad (12)$$

This is analogous to how imposing the radiation gauge in electromagnetism on each time slice leads to an elliptic equation for the scalar potential (see Smarr and York, 1978a).

The time slicing condition in equation (12) is termed "maximal slicing" in the literature, because it maximizes the volume of the 3-space relative to other slicings. Its major practical advantage is that it allows the evolution to penetrate inside of black holes, while slowing down the evolution in those regions enough to almost always avoid hitting singularities [see, e.g. Estabrook, et al. 1973; Smarr and York, 1978b; Eardley and Smarr, 1979; Shapiro and Teukolsky, 1980; Evans, 1984a,b]. Other possible slicings are discussed in Smarr and York, 1978b; Smarr, 1979; Eardley, 1979; Smarr, Taubes, and Wilson, 1980; Nakamura, 1981; and Bardeen and Piran, 1983.

With the time slicing set by the choice of the lapse function, one has to decide how to move the spatial coordinates from one slice to the next by choosing the shift vector. This choice is secondary to the choice of the time slicing, because if a bad time slice hits a singularity, then no further evolution is possible. However, given a good time slicing, one can lay spatial coordinates down on it using a variety of shift vectors. Equation (4) can be used to determine the conditions on β_i which must hold on each time level to enforce the desired coordinate condition. A rather complete discussion of the alternatives exists in the literature (Smarr and York, 1978b; Smarr, 1979; Wilson, 1979; Smarr, Taubes, and Wilson, 1980; Bardeen and Piran 1983; and Evans 1984b), as well as comparisons of different shift vectors used on the same time slicing (Eppley, 1979; Piran, 1980). One particular choice will be illustrated in section 3.

In summary, the Einstein equations yield a quasilinear system of evolution equations for (γ_{ij}, K_{ij}), which are intimately coupled to a set of (typically) elliptic equations for (α, β_i). The solutions to one set of equations are coefficients in the other set of equations, and vice versa. Therefore, they must be solved together, step by step into the future. This requirement of solving for the spacetime coordinates, simultaneously with the physical variables being evolved in those coordinates, is the major conceptual and numerical difference from ordinary flatspace problems.

c) Initial value equations and constraints

As mentioned above, the evolution equations (4) and (5) are only part of Einstein's equations. They are the analogs to the Maxwell equations for the time derivatives of the electric and magnetic fields (see e.g. Smarr and York, 1978a). However, there are also analogs of the constraint equations $D^iE_i = 4\pi\rho$ and $D_iB^i = 0$, which contain no time derivatives. The direct analog is the linear momentum constraint equation:

$$D^i[K_{ij} - \gamma_{ij}tr(K)] = 8\pi S_j. \tag{13}$$

Because gravity is spin-2 instead of spin-1 like electromagnetism, there is an extra index on the constraint equation. In addition, there is a nonlinear constraint equation in general relativity which has no direct analog in electromagnetism, termed the Hamiltonian constraint:

$$R^i{}_i + [tr(K)]^2 - K_{ij}K^{ij} = 16\pi\rho_H. \tag{14}$$

The existence of the constraint equations means that not all components of (γ_{ij}, K_{ij}) are true dynamical degrees of freedom (just as for A_i in electromagnetism). There are twelve functions in the pair (γ_{ij}, K_{ij}). Four of these can be fixed by the coordinate conditions imposed on (α, β_i). Four more are fixed by the four constraint equations. This leaves two free functions in each of γ_{ij} and K_{ij}. These represent the two degrees of freedom possessed by a propagating transverse gravitational wave field.

There are two fundamentally different ways to evolve numerically the Einstein equations (see Piran, 1980, for a complete discussion). The unconstrained evolution solves equations (4) and (5) for (γ_{ij}, K_{ij}) and inserts them into equations (13) and (14) as a check on the accuracy of the evolution. The constrained evolution uses equations (13) and (14) to solve for certain constrained pieces of (γ_{ij}, K_{ij}), while using a subset of equations (4) and (5) to evolve "dynamical" components of (γ_{ij}, K_{ij}). It is an unsolved problem as to which method is superior. Bardeen and Piran (1983) describe a partially constrained evolution scheme.

Our method, given below, uses the fully constrained approach (see Evans 1984a,b).

When the constraint equations are written in the form of equations (13) and (14), they are not very useful for numerical work, although some attempts have been made to use them (see Piran, 1980). An elegant method (see, e.g. York, 1979) from a theoretical as well as a numerical perspective, is to recast equations (13) and (14) as elliptic equations on "longitudinal" pieces of (γ_{ij}, K_{ij}). The 3-metric is split into a conformal factor ϕ and a conformally related 3-metric:

$$\gamma_{ij} = \phi^4 \hat{\gamma}_{ij}. \tag{15}$$

The conformal factor is the "Newtonian" part of the gravitational field, which determines the mass of the gravitating system, while the conformally related metric contains the gravitational radiation information (York 1971, 1972). The extrinsic curvature is scaled by the conformal transformation as

$$K^{ij} = \phi^{-10} \hat{K}^{ij} \tag{16}$$

and split into transverse and longitudinal parts:

$$\hat{K}^{ij} = \hat{K}_T^{ij} + \hat{K}_L^{ij}. \tag{17}$$

In what follows we assumed maximal slicing is applied. The longitudinal part can be derived from a vector potential W^i:

$$\hat{K}_L^{ij} = (\hat{L}W)^{ij} = \hat{D}^i W^j + \hat{D}^j W^i - 2/3\, \hat{\gamma}^{ij} \hat{D}_k W^k. \tag{18}$$

Here $\hat{D}_i$ is the covariant derivative built from $\hat{\gamma}_{ij}$.

The procedure to solve for a constrained initial data 3-space is as follows (York, 1979; Evans, 1984a,b). First, pick the unconstrained data $(\hat{\gamma}_{ij}, \hat{K}_T^{ij})$ and the "bare" matter variables (ρ_H, S^i). By substitution of equations (15), (16), (17), and (18) into equation (13) one transforms the momentum constraint into a linear vector elliptic equation:

$$(\hat{\Delta}_L W)^i = \hat{D}_j (\hat{L}W)^{ij} = \hat{D}_k \hat{D}^k W^i + 1/3\, \hat{D}^i (\hat{D}_k W^k) + \hat{R}_k^i W^k = 8\pi \hat{S}^i, \tag{19}$$

which one solves for the potential W_i. Here, $\hat{R}_{ij}$ is the Ricci tensor built out of $\hat{\gamma}_{ij}$. With $\hat{K}_T^{ij}$ and W_i, one can construct $\hat{K}^{ij}$, using equations (17) and (18). Substituting equations (15) and (16) into equation (14) one transforms the Hamiltonian constraint into a quasilinear elliptic equation:

$$\hat{\Delta}\,\phi = (\phi/8)\,[\hat{R}_i{}^i - 16\pi\,\hat{\rho}_H\,\phi^{-2} - (\hat{K}_{ij}\hat{K}^{ij})\,\phi^{-8}], \qquad (20)$$

which one solves for the conformal factor. Here, $\hat{\Delta}$ is the covariant Laplacian built out of $\hat{\gamma}_{ij}$. The conformal factor ϕ can now be used to "dress" all the "bare" free data by equation (15), (16) and:

$$\rho_H = \phi^{-6}\,\hat{\rho}_H\,, \quad S^i = \phi^{-10}\,\hat{S}^i\,. \qquad (21)$$

By construction, the data (γ_{ij}, K_{ij}, ρ_H, S^i), now satisfies the constraint equations. How this scheme can be used to provide a constrained evolution, will be the subject of section 3.

Our emphasis will not be on the astrophysical significance of the calculations, but rather on the form of the Einstein equations and how one can finite difference them. We will only discuss our dynamical axisymmetric code. For descriptions of the three possible one-spatial dimensional codes see: spherical (Misner and Sharp, 1964; May and White, 1967; Estabrook, et al. 1973; Wilson, 1979; Shapiro and Teukolsky, 1979, 1980), planar (Centrella and Wilson, 1983, 1984), and cylindrical (Piran, 1980). For discussions of other two-spatial dimension relativity codes see e.g. Smarr, 1975; Smarr, 1979; Smarr, 1984; Eppley, 1979; Nakamura, et al. 1980; Nakamura, 1981; and Bardeen and Piran, 1983.

3. AXISYMMETRIC MODEL

a) Symmetries, gauge, and differential equations

In this section we describe the equations and numerical method used in a computer code we have developed to study, in a fully self-consistent manner, general relativistic hydrodynamic systems. Our calculation is restricted to configurations exhibiting axisymmetry, no axial rotation, and equatorial plane symmetry. This discussion is intended to provide an update on some of the progress we have made since Wilson (1979) and Dykema (1980). The emphasis here is on presenting for the numerical astrophysicist the form of the differential equations to be solved and a survey of the numerical techniques employed, particularly several new aspects, which have allowed us to obtain stable and regular solutions. A more complete description of the mathematical algorithm can be found in Evans (1984a,b) which includes the hydrodynamic equations not given here.

A numerical method for calculating axisymmetric models has been presented previously (Wilson, 1979) using cylindrical spatial coordinates (ρ, z, ϕ). Shortly thereafter we switched to using spherical coordinates (r, θ, ϕ) which are better suited to the study of black hole formation (Dykema, 1980). While cylindrical

coordinates would be better for calculating a two neutron star collision, the new code can be used to simulate problems such as the bounce of aspherical neutron stars, the collapse of stars to form black holes, and the formation of black holes by pure gravity waves (Brill, 1959). The reason for this change has been the need to well cover the "throat" which forms in the interior of the black hole once an horizon appears. The proper length of the throat increases monotonically with external time, forcing us to put more of our grid points into the black hole (Estabrook, et al. 1973; Shapiro and Teukolsky, 1980).

These collapse calculations are very "stiff"; there are disparate length scales in the problem which require many zones to accurately simulate. For example in the exterior of a newly formed black hole, the gravitational radiation emitted during the ring down has a far field wavelength of approximately 20M where M is the mass of the hole. It is necessary therefore to have the grid extend out to a distance on the order of 100M in order to be able to analyze the radiation in the wave zone. When the black hole forms, the coordinate radius of the surface of the collapsing star goes to zero exponentially with external time. This effect is due to an impending coordinate singularity brought about by our 3-gauge choice combined with maximal slicing. Maximal slicing exponentially slows the advance of proper time which effectively freezes the star at a finite proper radius. Nonetheless the interior of the star must be well zoned which requires many radial zones to span the two regions. This represents an extreme situation which our code must handle. For further discussion of the crucial role of accuracy and grid resolution see Smarr (1984).

The methods used for solving the hydrodynamic equations have been virtually unchanged, despite the new coordinates, since Wilson (1979). However, the techniques to solve for components of the gravitational field have undergone significant revision. We will therefore only discuss these techniques, which are rather different from those described in Wilson (1979), used in the new code for the solution of the gravitational field.

The time coordinate is chosen by employing maximal slicing, equation (12). In addition, we pick the spatial coordinate gauge by choosing conditions on the shift vector which fix the form of the 3-metric in time. There are several choices of this type and the one we have used fixes the form of the line element to be:

$$ds^2 = -\alpha^2 dt^2 + A^2(dr + \beta^r dt)^2 + A^2 r^2(d\theta + \beta^\theta dt)^2 + B^2 r^2 \sin^2\theta \, d\phi^2, \qquad (22)$$

where boundary conditions are employed to make (r, θ, ϕ) spherical coordinates. The advantage of such simplifying gauges is that the

shift can be used to minimize the number of independent components in the 3-metric, which vastly simplifies the number of terms involved in calculating 3-covariant derivatives.

The constraint equations (13) and (14) are superfluous during an evolution in the sense that once they have been used to obtain consistent initial data, the evolution equations (4) and (5) guarantee their continued satisfaction at subsequent times. Numerically this will not be true, as the degree to which the constraints are satisfied tends to decrease with time due to numerical drift. Since we do not understand the stability of non-Einstein data (data off the constraint surface), we have chosen to invert all the constraint equations on each successive time level and evolve a reduced dynamical problem (fully constrained approach). The constrained approach, using a simplifying gauge choice has the further advantage that the number of evolved components of the gravitational field will reflect precisely the number of dynamical degrees of freedom. We can therefore choose to evolve components which are closely related to gravitational radiation variables in the weak field, wave zone. With our symmetries only one dynamical degree of freedom exists (one independent polarization state) and the component of the metric we evolve is immediately relatable to the weak field transverse-traceless gravitational radiation amplitude h_+^{TT} $(r \pm t, \theta, \phi)$ (Evans, 1984b).

The technique used for solving the momentum constraints uses the full York (1973) transverse-traceless decomposition of the extrinsic curvature tensor. This includes inverting a transverse part, ordinarily not done on the initial slice, but which must be done on subsequent time slices to provide the fully constrained approach. In addition, the solution for the longitudinal part on the initial slice provides more physically meaningful initial data.

In what follows we give the equations for the gravitational field in the form most appropriate for finite differencing. The presentation of the differential equations will be brief since their derivation can be found elsewhere (Evans, 1984a,b). Also we do not discuss here the hydrodynamic equations of motion, though hydrodynamic quantities will enter as source terms in the other equations. Of the possible metric simplifying gauges, the choice (22) places the metric in diagonal and quasi-isotropic form (reduces for a static spherical configuration to the isotropic coordinates for Schwarzschild geometry). This amounts to demanding that $\partial_t \gamma_{r\theta} = \partial_t [r^2\gamma_{rr} - \gamma_{\theta\theta}] = 0$ and that $\gamma_{r\theta} = r^2\gamma_{rr} - \gamma_{\theta\theta} = 0$ on the initial slice, since $\gamma_{r\phi} = \gamma_{\theta\phi} = 0$ due to the symmetry assumptions. The 3-metric with the definitions $\gamma_{rr} = A^2$ and $\gamma_{\phi\phi} = B^2r^2\sin^2\theta$ then has the form

$$\gamma_{ij} = \text{diag}\ (A^2,\ A^2r^2,\ B^2r^2\sin^2\theta), \tag{23}$$

though we also use the alternative form,

$$\gamma_{ij} = \phi^4\ \text{diag}\ (T^{2/3},\ T^{2/3}r^2,\ T^{-4/3}r^2\sin^2\theta) = \phi^4\ \hat{\gamma}_{ij}, \tag{24}$$

with the definition

$$\phi^6 = A^2B \quad , \quad T = \frac{A}{B}\ . \tag{25}$$

The metric $\hat{\gamma}_{ij}$ is the conformally related metric for which $[\det\ (\hat{\gamma}_{ij})]^{1/2} = r^2\sin\theta$, ϕ is the conformal factor used for all conformal scalings, and lnT, which vanishes in spherical symmetry, gives a measure of the anisotropy of the 3-space.

The gauge conditions which allow the metric to be written in the form (23) fix two relationships between the shift components β^r and β^θ ($\beta^\phi = 0$ with no rotation). These are

$$r\,\partial_r\left(\frac{\beta^r}{r}\right) - \partial_\theta\beta^\theta = \alpha\,(2\,K^r_r + K^\phi_\phi)\ , \tag{26}$$

$$r\,\partial_r\,\beta^\theta + \partial_\theta\left(\frac{\beta^r}{r}\right) = 2\,\alpha\,\frac{K^r_\theta}{r}\ . \tag{27}$$

This first order system of partial differential equations (PDE) is elliptic (Evans 1984b). This system is not directly numerically inverted but rather is rewritten as a pair of second order PDEs. Potentials, χ and Φ, are introduced by

$$\frac{\beta^r}{r} = r\,\partial_r\,\chi + \partial_\theta\,\Phi, \tag{28}$$

$$\beta^\theta = r\,\partial_r\,\Phi - \partial_\theta\,\chi, \tag{29}$$

which allow (26) and (27) to be written as separate second order equations

$$\frac{1}{r}\,\partial_r(r\,\partial_r\chi) + \frac{1}{r^2}\,\partial_\theta\partial_\theta\chi = \frac{\alpha}{r^2}\,(2\,K^r_r + K^\phi_\phi), \tag{30}$$

$$\frac{1}{r}\,\partial_r(r\,\partial_r\Phi) + \frac{1}{r^2}\,\partial_\theta\partial_\theta\Phi = \frac{2\alpha}{r^2}\left(\frac{K^r_\theta}{r}\right)\ , \tag{31}$$

where the differential operators are flat space 2-dimensional Laplacians. With our assumed symmetries the numerical calculation is carried out over the single quadrant $0 \leq \theta \leq \pi/2$ in the (r,θ) plane. The angular boundary conditions for χ and Φ are $\partial_\theta\chi = \Phi =$

0 for $\theta = 0, \pi/2$. The radial boundary conditions at $r = 0$ and at large radius will be left until the numerical techniques for treating this system are described below.

We give the evolution equations for the metric components ϕ and lnT, derived from the general evolution equations (4) and (5), though in our approach only the component lnT is directly evolved, with ϕ found by solving the Hamiltonian constraint on successive time slices. These are,

$$\partial_t(\phi^6) = \frac{1}{r^2}\partial_r\,[r^2\phi^6\beta^r] + \frac{1}{\sin\theta}\partial_\theta\,[\sin\theta\ \phi^6\beta^\theta], \tag{32}$$

$$\partial_t \ln T = \beta^r\partial_r \ln T + \beta^\theta\partial_\theta \ln T + \partial_\theta\beta^\theta - \cot\theta\ \beta^\theta + \alpha\ \lambda, \tag{33}$$

where $\lambda = K^r_r + 2\ K^\phi_\phi$ is a particular linear combination of the extrinsic curvature tensor which we have found useful.

With our assumed symmetries and maximal slicing only the three components K^ϕ_ϕ, λ, and K^r_θ of the extrinsic curvature are independent. Using equations (5) and (32) we evolve the conformally related quantity $\hat{\lambda} = \phi^6\lambda$ by,

$$\begin{aligned}\partial_t\,\hat{\lambda} = {} & \frac{1}{r^2}\partial_r(r^2\beta^r\hat{\lambda}) + \frac{1}{\sin\theta}\partial_\theta(\sin\theta\ \beta^\theta\ \hat{\lambda}) \\ & + \frac{\hat{K}^r_\theta}{r}\left[r\partial_r\beta^\theta - \partial_\theta\left(\frac{\beta^r}{r}\right)\right] + \frac{8\,\pi\,\alpha\,B\,S^2_\theta}{r^2(D + E + pU)U} \\ & + \frac{1}{r^2}\partial_r[r^2\alpha\ B\partial_r \ln T] + \frac{AB^2\sin\theta}{r^2}\partial_\theta\left[\frac{1}{AB\sin\theta}\partial_\theta\alpha\right] \\ & + \frac{\alpha B^2\sin\theta}{r^2}\partial_\theta\left[\frac{1}{AB\sin\theta}\partial_\theta A\right],\end{aligned} \tag{34}$$

where D, E, S_θ, p, and U are hydrodynamic quantities (Evans, 1984a,b; Dykema, 1980) and alternate metric variables are used to provide the simplest result. Note that λ and lnT satisfy the boundary conditions $\partial_\theta\lambda = 0$ for $\theta = 0, \pi/2$, $\partial_r\lambda = 0$ at $r = 0$, and an outgoing radiation (Sommerfeld) condition is applied at $r = r_m$.

We also obtain from equation (12) the elliptic lapse equation for α due to the maximal slicing conditions $\partial_t\,tr(K) = tr(K) = 0$:

$$\frac{1}{r^2}\,\partial_r[r^2 B\,\partial_r\alpha] + \frac{1}{\sin\theta}\,\partial_\theta[\sin\theta\; B\,\partial_\theta\alpha]$$

$$= \alpha\,\phi^6\{2\lambda^2 - 6\lambda(K^\phi_\phi) + 6(K^\phi_\phi)^2 + 2\,(\frac{K^r_\theta}{r})^2 \tag{35}$$

$$+ 8\pi\,(D + E)\,(U - \frac{1}{2U}) + 8\pi\,pU(U + \frac{1}{2U})\}.$$

The lapse satisfies boundary conditions $\partial_\theta\alpha = 0$ for $\theta = 0,\ \pi/2$, $\partial_r\alpha = 0$ at $r = 0$. The exterior condition at large radius is discussed in Evans (1984b).

The Hamiltonian constraint (20) would ordinarily be written as an equation for the conformal factor ϕ, but we use it instead to solve for the metric component $\psi \equiv B^{1/2}$, where the two are related by $\phi^6 = T^2\psi^6$. The source of the Hamiltonian constraint is written in terms of conformally related quantities $\hat{K}^i_j$, D, E and the metric T which are already obtained. The quasilinear elliptic equation becomes,

$$\frac{1}{r^2}\,\partial_r(r^2\partial_r\phi) + \frac{1}{r^2\sin\theta}\,\partial_\theta(\sin\theta\;\partial_\theta\phi)$$

$$= -\frac{1}{4}\,\psi\,[\frac{1}{r}\,\partial_r(r\partial_r\,\ln T) + \frac{1}{r^2}\,\partial_\theta\partial_\theta\,\ln T \tag{36}$$

$$+ T^{-2}\psi^{-8}(\hat{\lambda}^2 - 3\hat{\lambda}\hat{K}^\phi_\phi + 3\hat{K}^\phi_\phi{}^2 + (\frac{\hat{K}^r_\theta}{r})^2)$$

$$+ 8\pi\,\phi^{-2}\hat{D}U + 8\pi\,T^{2(1-\Gamma)}\,\phi^{4-6\Gamma}\,\hat{E}(\Gamma U + \frac{1-\Gamma}{U})],$$

where Γ is the ratio of specific heats. The equation in this form can be used for solution of the initial value problem as well as on subsequent time slices. This is in fact the reason conformally related quantities are evolved instead of the physical values. The boundary conditions used are: $\partial_\theta\phi = 0$ at $\theta = 0,\ \pi/2$, $\partial_r\psi = 0$ at $r = 0$, and the Robin condition $\partial_r\phi + \frac{1}{r}\,(\phi-1)\big|_{r=r_m} = 0$ (York and Piran, 1982). Once the Hamiltonian constraint is solved and ϕ is known, the physical quantities are obtained by their respective

conformal scalings: $K^i_j = \phi^{-6}\,\hat{K}^i_j$, $S_i = \phi^{-6}\,\hat{S}_i$, $D = \phi^{-6}\,\hat{D}$, and $E = \phi^{-6\Gamma}\,\hat{E}$.

We evolve only one component of the extrinsic curvature; the other two are obtained by inversion of the momentum constraints [see equation (13)]. The conformally related extrinsic curvature $\hat{K}^i_j = \phi^6 K^i_j$ is decomposed into transverse and longitudinal parts using (17), with the transverse part satisfying $D_i \hat{K}^i_{Tj} = 0$. The vector potential W_i for the longitudinal part of $\hat{K}^i_j$ is obtained by solution of the second order elliptic "vector Laplacian" (York, 1973, 1979), equation (19). Since $W^\phi = S_\phi = 0$, this system yields two coupled equations:

$$\frac{4}{3}\frac{1}{r^2}\partial_r[r^4\partial_r(\frac{W^r}{r})] + \underline{\frac{1}{\sin\theta}\partial_\theta[\sin\theta\,\partial_\theta(\frac{W^r}{r})]} + F_1(\frac{W^r}{r})$$

$$+ \frac{r}{3T^2\sin\theta}\partial_\theta[T^2\sin^2\theta\cos\theta\,\partial_r(\frac{W^\theta}{\sin\theta\cos\theta})] \qquad (37)$$

$$- \frac{2}{3}\sin\theta\cos\theta\,(3 + \frac{r}{T}\partial_r T)\,\partial_\theta(\frac{W^\theta}{\sin\theta\cos\theta})$$

$$+ F_2(\frac{W^\theta}{\sin\theta\cos\theta}) = 8\pi\, r\,\hat{S}_r,$$

$$\frac{\sin\theta\cos\theta}{r^2}\partial_r[r^4\partial_r(\frac{W^\theta}{\sin\theta\cos\theta})]$$

$$+ \frac{4}{3}\frac{1}{\sin^2\theta\cos\theta}\partial_\theta[\sin^3\theta\cos^2\theta\,\partial_\theta(\frac{W^\theta}{\sin\theta\cos\theta})] + \underline{F_3(\frac{W^\theta}{\sin\theta\cos\theta})}$$

$$+ \frac{1}{3}\,r\,T^2\,\partial_\theta[\frac{1}{T^2}\partial_r(\frac{W^r}{r})] + \underline{(3 + \frac{2}{3}\frac{r}{T}\partial_r T)\,\partial_\theta(\frac{W^r}{r})} \qquad (38)$$

$$+ F_4(\frac{W^r}{r}) = 8\pi\,\hat{S}_\theta,$$

with

$$F_1 = \frac{2}{3}\frac{T^2}{r^2}\partial_r[\frac{r^4}{T^3}\partial_r T],$$

$$F_2 = \underline{-4 + 6\sin^2\theta} + \frac{2}{3}\frac{r}{T}\partial_r T + \frac{2}{3}\frac{T^2\sin\theta\cos\theta}{r^2}\partial_r[\frac{r^3}{T^3}\partial_\theta T], \qquad (39)$$

$$F_3 = \underline{-6\sin\theta\cos\theta} + \frac{2}{3}\frac{T^2\cos\theta}{\sin^4\theta}\partial_\theta\left[\frac{\sin^5\theta}{T^3}\partial_\theta T\right],$$

$$F_4 = \frac{2}{3}\frac{T^2 r}{\sin^3\theta}\partial_\theta\left[\frac{\sin^3\theta}{T^3}\partial_r T\right].$$

These equations are written in a form different from Evans (1984a) as the form given here is appropriate for finite differencing. Also, the underlined terms are for later reference in considering how to best difference this system.

Once W^r and W^θ are known, the longitudinal components are obtained from (18)

$$\hat{\lambda}_L = -\frac{2r}{T}\partial_r T\left(\frac{W^r}{r}\right) - \frac{2\sin\theta}{T}\partial_\theta\left[T\cos\theta\left(\frac{W^\theta}{\sin\theta\cos\theta}\right)\right], \tag{40}$$

$$\hat{K}_{L\phi}^{\ \phi} = -\frac{2}{3}\frac{r}{T^2}\partial_r\left[T^2\left(\frac{W^r}{r}\right)\right] - \frac{2}{3}\frac{\sin^2\theta}{T^2}\partial_\theta\left[T^2\cot\theta\left(\frac{W^\theta}{\sin\theta\cos\theta}\right)\right], \tag{41}$$

$$\frac{\hat{K}_{L\theta}^{\ r}}{r} = \partial_\theta\left(\frac{W^r}{r}\right) + r\sin\theta\cos\theta\,\partial_r\left(\frac{W^\theta}{\sin\theta\cos\theta}\right). \tag{42}$$

Since $\hat{\lambda}$ has been evolved, equations (17) and (40) give the transverse part of $\hat{\lambda}$ by $\hat{\lambda}_T = \hat{\lambda} - \hat{\lambda}_L$. The transverse part of $\hat{K}_j^{\ i}$, which satisfies $\hat{D}_j\hat{K}_T^{\ j}{}_i = 0$, is also identically the solution of the second order elliptic system, the "tensor Laplacian" (Evans, 1984a,b; York, 1973),

$$(\hat{\Delta}_T\hat{K}_T)_j^{\ i} \equiv [\hat{L}(\hat{D}\cdot\hat{K}_T)]_j^{\ i} = 0. \tag{43}$$

Taking the (r,r) and (r,θ) components, this reduces to two coupled PDEs for $\hat{K}_{T\phi}^{\ \phi}$ and $\hat{K}_{T\theta}^{\ r}$ using $\hat{\lambda}_T$ as source:

$$4T^{2/3}\partial_r\left[\frac{r^2}{T^{2/3}}\partial_r\hat{K}_{T\phi}^{\ \phi}\right] + \frac{T^{2/3}}{\sin\theta}\partial_\theta\left[\frac{\sin\theta}{T^{2/3}}\partial_\theta\hat{K}_{T\phi}^{\ \phi}\right] + \underline{G_1\hat{K}_{T\phi}^{\ \phi}}$$

$$- \frac{r}{T^{5/3}\sin\theta}\partial_\theta\left[\sin^2\theta\cos\theta\,T^{5/3}\partial_r\left(\frac{\hat{K}_{T\theta}^{\ r}}{r\sin\theta\cos\theta}\right)\right]$$

$$+ \left(7 + \frac{r}{3T}\partial_r T\right)\sin\theta\cos\theta\,\partial_\theta\left(\frac{\hat{K}_{T\theta}^{\ r}}{r\sin\theta\cos\theta}\right) + \underline{G_2\left(\frac{\hat{K}_{T\theta}^{\ r}}{r\sin\theta\cos\theta}\right)}$$

$$= 2\,T^{1/6}\sin^2\theta\,\partial_r\left[\frac{r^2}{T^{1/6}}\,\partial_r\left(\frac{\hat{\lambda}_T}{\sin^2\theta}\right)\right] + \sin^2\theta\,\partial_\theta\partial_\theta\left(\frac{\hat{\lambda}_T}{\sin^2\theta}\right)$$

$$+ G_3\left(\frac{\hat{\lambda}_T}{\sin^2\theta}\right), \tag{44}$$

$$T^{2/3}\sin\theta\cos\theta\,\partial_r\left[\frac{r^2}{T^{2/3}}\,\partial_r\left(\frac{\hat{K}^r_{T\theta}}{r\sin\theta\cos\theta}\right)\right]$$

$$+ \frac{T^{2/3}}{\sin^2\theta\cos\theta}\,\partial_\theta\left[\frac{\sin^3\theta\cos^2\theta}{T^{2/3}}\,\partial_\theta\left(\frac{\hat{K}^r_{T\theta}}{r\sin\theta\cos\theta}\right)\right] + G_4\left(\frac{\hat{K}^r_{T\theta}}{r\sin\theta\cos\theta}\right)$$

$$-rT^{7/3}\partial_\theta\left[T^{-7/3}\partial_r\hat{K}^\phi_{T\phi}\right] + \left(-8 + \frac{r}{3T}\,\partial_r T\right)\partial_\theta\hat{K}^\phi_{T\phi} + G_5\,\hat{K}^\phi_{T\phi}$$

$$= \left(\sin\theta\cos\theta + \frac{2}{3}\sin^2\theta\,\frac{1}{T}\,\partial_\theta T\right) r\partial_r\left(\frac{\hat{\lambda}_T}{\sin^2\theta}\right)$$

$$- \left(5 + \frac{2r}{3T}\,\partial_r T\right)\sin^2\theta\,\partial_\theta\left(\frac{\hat{\lambda}_T}{\sin^2\theta}\right) + G_6\left(\frac{\hat{\lambda}_T}{\sin^2\theta}\right), \tag{45}$$

with

$$G_1 = 12\,r^3\,T^{1/6}\,\partial_r\left[\frac{1}{r^2}\,\partial_r\left(\frac{r}{T^{1/6}}\right)\right] + \frac{T^{5/3}}{\sin\theta}\,\partial_\theta\left[\frac{\sin\theta}{T^{8/3}}\,\partial_\theta T\right],$$

$$G_2 = (3\cos^2\theta - 1)\left(7 + \frac{r}{3T}\,\partial_r T\right) - 5\sin\theta\cos\theta\,\frac{1}{T}\,\partial_\theta T,$$

$$G_3 = \underline{6\cos^2\theta - 15\sin^2\theta} - 5\sin\theta\cos\theta\,\frac{1}{T}\partial_\theta T - r\sin^2\theta\,\frac{1}{T}\partial_r T\ ,$$

$$G_4 = -\sin\theta\cos\theta\,[\underline{12} + \frac{2r}{T}\partial_r T + \frac{2}{3}(2\cot\theta - \tan\theta)\,\frac{1}{T}\partial_\theta T]\ ,$$

$$G_5 = r^3 T^{2/3}\,\partial_r\,[\frac{1}{r^2 T^{5/3}}\partial_\theta T] - \frac{3T^{2/3}}{r}\partial_\theta\,[\frac{1}{T^{1/3}}\partial_r\,(\frac{r^2}{T^{1/3}})]\ ,$$

$$G_6 = \underline{-12\sin\theta\cos\theta} + 2\sin^2\theta\,\frac{1}{T}\partial_\theta T - 2r\sin\theta\cos\theta\,\frac{1}{T}\partial_r T. \qquad (46)$$

The boundary conditions for $\hat{K}^{\phi}_{T\phi}$ and $\hat{K}^{r}_{T\theta}$ are $\hat{K}^{r}_{T\theta} = \partial_\theta \hat{K}^{\phi}_{T\phi} = 0$ for $\theta = 0,\ \pi/2$, $\partial_r \hat{K}^{\phi}_{T\phi} = \partial_r(\frac{\hat{K}^{r}_{T\theta}}{r}) = 0$ at $r = 0$, and an approximate weak field transverse-traceless radiation boundary condition at $r = r_m$: $\hat{K}^{\phi}_{T\phi}(r_m) = \frac{1}{2}\hat{\lambda}_T(r_m)$, $\hat{K}^{r}_{T\theta}(r_m) \approx 0$ (Evans 1984b). Having evolved only $\hat{\lambda}$, $\hat{S}_r$ and $\hat{S}_\theta$, the entire (conformal) extrinsic curvature tensor has now been reconstructed.

The equations (37), (38) and (44), (45) are rather complicated but their use allows the momentum constraints (13) to be represented by second order elliptic systems. The foremost reasons for their use is that 1) the solution of (37) and (38) for the initial value problem provides physically more interestng initial data and that 2) the use of second order equations allows iterative numerical matrix inversion techniques to be applied and the proper (asymptotic) boundary conditions to be formulated.

b) Finite differencing

The numerical algorithm employed is a time explicit, Eulerian scheme utilizing a partially adaptive mesh. The calculation is approximately second order accurate in the two spatial directions (deviations due to a graded mesh in the radial direction) and generally first order accurate in time (though transport is largely second order accurate).

The single quadrant of the (r,θ) plane over which the calculation is performed is zoned by giving the discrete set of radii r_j and angles θ_k for zone corners with $1 \le j \le jm$ and $1 \le k \le km$. The

angles are fixed by $\theta_{k=2} = 0$, $\theta_{k=km} = \pi/2$ and use of equal angular increments $\Delta\theta$. In addition, zone centered angles are given by $\theta_{k+1/2}$ where $\theta_{k+1/2} = \theta_k + 1/2\ \Delta\theta$ and dummy zone centers at $\theta_{3/2}$ and $\theta_{km+1/2}$ are employed to facilitate application of angular boundary conditions. Radial positions of zone corners are given by a graded mesh $r_{j+1} = r_j + \Delta r_{j+1/2}$ with, typical, $\Delta r_{j+1/2} > \Delta_{j-1/2}$ where $\Delta r_{j+1/2}$ is the zone width between faces at j and j+1. These positions are altered during the calculation to put radial zones where they are needed and leads to an associated grid velocity, $V_g{}^r$. Two radial locations remain fixed: $r_2 = 0$ and $r_{jm} = r_m$. A set of zone centered positions $r_{j+1/2}$ are carried as well with $r_{j+1/2} = 1/2(r_j + r_{j+1})$ and associated widths Δr_j such that $r_{j+1/2} = r_{j-1/2} + \Delta r_j$. Dummy zone centers are located at $r_{3/2}$ and $r_{jm+1/2}$.

In many situations there will be disparate physical length scales that require $r_{jm}/r_3 > jm$ (jm the number of alloted radial zones). This necessitates a graded mesh and we (usually) use a uniform grading $\Delta r_{j+1/2} = \sigma\ \Delta r_{j-1/2}$, σ = constant. The constant is determined initially by specifying r_3 and r_{jm}. To generate the mesh on a new slice, r_3 typically is changed to roughly track the material compression in the inner-most zone:

$$r_3{}^{n+1} = r_3{}^n + \xi\ \bar{V}_3{}^r \Delta t\ , \qquad \xi \cong 1.0, \tag{47}$$

where $\bar{V}_3{}^r$ is the average material velocity in the first zone. Then the new value of r_3 is used with r_{jm} (held fixed) to obtain a new σ, which generates the new mesh $(r_j, r_{j+1/2})$. Finally, a grid velocity is produced by

$$V_g{}^r{}_j = \frac{1}{\Delta t}\,(r_j{}^{n+1} - r_j{}^n), \tag{48}$$

which is included in all evolution equations as giving a hydrodynamic-like convective derivative (Dykema 1980). This method of continuous remapping maintains well resolved, smooth zoning, even in the interior of black holes.

The natural spatial centering from the difference equations considers the following variables as zone centered: the hydrodynamic quantities D, E, p and U; the gravitational field quantities T, ϕ, λ, α, $K^{\phi}{}_{\phi}$, and the alternate metric set A and B. The variables centered on radial zone interfaces (r_j) are S_r, V^r, V_g^r, β^r, and W^r. Those centered on angular zone interfaces (θ_k) are S_θ, V^θ, β^θ, and W^θ. Finally, $K^r{}_\theta$ is naturally centered at the zone corners (θ_k, r_j). The time centering of velocity-like vari-

ables i.e., λ, $K^{\phi}{}_{\phi}$, $K^{r}{}_{\theta}$, S_r, S_θ, V^r, $V^r{}_g$, β^r, β^θ can be thought of at a time level $\Delta t/2$ offset from all others. Operator splitting is used extensively throughout the code, though we will not explicitly indicate the details here (see Dykema 1980 for further details).

We will treat some of the numerical issues in what follows. Our method for handling the transport terms that appear in the evolution equations for the gravitational field, (33) and (34), is briefly described. We use for these equations a transport scheme very similar to that used for the hydrodynamic equations (Dykema 1980; Wilson 1979) and a more complete discussion can be found in Dykema (1980). We then concentrate on discussing a number of questions surrounding the finite differencing of the various elliptic equations that arise from our analytic method. We do not present the complete difference equations in each case since many aspects of the differencing and averaging are largely arbitrary. Rather, we will devote attention to the general techniques used except for those points which have been developed which have contributed significantly to obtaining stable, regular results.

The first step in updating the dynamical quantities λ and $\ln T$ to a succeeding time level is to advance the values at the outer boundary. Here the boundary condition is modeled as an outgoing spherical wave,

$$\partial_t \hat{\lambda} = -\frac{c}{r}\,\partial_r(r\hat{\lambda}) \tag{49}$$

where $c = -\beta^r + \alpha/A$ is the local speed of light. The difference equation becomes (with angular index suppressed)

$$\hat{\lambda}^{\,n+1}_{jm+1/2} = \hat{\lambda}^{\,n}_{jm+1/2} - c_{jm}\frac{\Delta t}{\Delta r_{jm}}\left[\hat{\lambda}^{n}_{jm+1/2} - \frac{r_{jm-1/2}}{r_{jm+1/2}}\,\hat{\lambda}^{n}_{jm-1/2}\right] \tag{50}$$

with c_{jm} computed at the zone interface. The use of (50) has typically resulted in a very low impedance mismatch; our gravity waves propagate off the mesh very cleanly. We handle $\ln T$ in a similar way.

The transport terms of equation (33) are differenced as follows. An update of $\ln T$ in the radial direction is accomplished by,

$$(\ln T)^{n+1}_{j+1/2} = (\ln T)^{n}_{j+1/2} + (\Delta t/2)\overline{V^r}_{j+1/2}\left[(\partial_r \ln T)^n_j\,(1-\eta_{j+1/2}) + (\partial_r \ln T)^n_{j+1}\,(1+\eta_{j+1/2})\right], \tag{51a}$$

where,

$$\bar{v}^r_{j+1/2} = 1/2[(\beta^r_j + v_{g\,i}{}^r) + (\beta^r_{j+1} + v_{g\,j+1}{}^r)], \tag{51b}$$

$$(\partial_r \ln T)^n_j = \frac{1}{\Delta r_j}\,[\ln T^n_{j+3/2} - \ln T^n_{j+1/2}], \tag{51c}$$

$$\eta_{j+1/2} = (1-\mu_{j+1/2})\,\frac{\Delta t \bar{v}^r_{j+1/2}}{\Delta r_{j+1/2}} + \mu_{j+1/2}\,\frac{\bar{v}^r_{j+1/2}}{|\bar{v}^r_{j+1/2}|}\,, \tag{51d}$$

$$\mu_{j+1/2} = \frac{|(\partial_r \ln T)^2_{j+1} - (\partial_r \ln T)^2_j|}{(\partial_r \ln T)^2_{j+1} + (\partial_r \ln T)^2_j} \tag{51e}$$

which is mixed first order, second order transport and the grid velocity (for the radial direction only) is evident. The transport in the θ-direction is immediately obtainable, however the combined update is accomplished by three sweeps through the mesh, updating partially $\Delta t/2$ in the radial direction, Δt in the θ-direction, and a final $\Delta t/2$ in the radial direction. This is due to the observation by Leith (1965) that the above method is von Neumann stable and formally more accurate.

A similar weighted first order, second order method is used for the transport terms in equation (34) for $\hat{\lambda}$, except these have the appearance of a divergence of a flux. Conservative differencing is employed so that the sum $\sum_{j,k} \hat{\lambda}_{k+1/2,j+1/2}\,(r^3_{j+1}-r^3_j)(\cos\theta_k-\cos\theta_{k+1})/3$ is maintained during the transport update. To do so, the relevant differential operators in (34) must be replaced according to

$$\frac{1}{r^2}\,\partial r\,\Big|_{j+1/2} \to \frac{3\Delta_{j+1/2}}{(r^3_{j+1}-r^3_j)}\,, \tag{52a}$$

$$\frac{1}{\sin\theta}\,\partial_\theta\,\Big|_{k+1/2} \to \frac{\Delta_{k+1/2}}{\cos\theta_k - \cos\theta_{k+1}}\,. \tag{52b}$$

The reader is referred to the complete discussion by Dykema (1980) for the finite difference equation for (34). More up-to-date transport algorithms could be used for both (33) and (34) as well as the relativistic hydrodynamics equations (see Hawley, Smarr, and Wilson (1984) for comparisons of these methods). The use of transport algorithms of this type for the gravitational field quantities stems from the conclusion that the transport will be mostly second order accurate since these fields show no tendancy to steepen, unlike the fluid, into shock-like structures.

The symmetry boundary conditions for $\hat{\lambda}$ are $\hat{\lambda}_{j=3/2} = \hat{\lambda}_{j=5/2}$ at

the origin, $\hat{\lambda}_{k=3/2} = \hat{\lambda}_{k=5/2}$ at $\theta=0$ and $\hat{\lambda}_{k=km-1/2} = \hat{\lambda}_{k=km+1/2}$ on the equator. Note that $\hat{\lambda} = 0$ on axis as well as satisfying $\partial_\theta \hat{\lambda} = 0$ there. Use of the Neumann conditions allows $\hat{\lambda}$ to drift near $\theta=0$, but in practice this is always relatively small. The conditions for lnT are the same except $(\ln T)_{k=5/2} = 0$ is maintained.

We turn next to the issue of finite differencing the elliptic systems. The equation (35) for the lapse function, α, is a straightforward scalar elliptic equation. There are no fundamental problems in obtaining solutions and we solve it by using successive over relaxation (SOR). In order to reduce the number of relaxation iterations, an extrapolation acceleration for α is used of the form

$$\alpha(t_n)_{\text{first guess}} = \frac{\alpha^2(t_{n-1})}{\alpha(t_{n-2})} . \tag{53}$$

This of course requires storing an extra time level. Geometrical extrapolation is used for α because once a black hole forms, α decreases exponentially in time in the strong field region (Smarr and York, 1978b; Evans, 1984a,b). The lapse is considered zone-centered and so the Neumann conditions on the axis, equator and at the origin are naturally applied as was done for $\hat{\lambda}$ above.

The Hamiltonian constraint (36), used to obtain the metric variable $w = B^{1/2}$, is nonlinear. To find its solution, we use a best available guess for ϕ to evaluate the source (the right-hand-side). Then the linear operator is solved by SOR to obtain a temporary function $\bar{\phi}$. The next approximation to the solution is formed by taking a weighted linear combination of $\bar{\phi}$ and the last guess. This is a modified Picard (outer) iteration. Writing equation (36) as $\Delta\phi = N(\phi)$, where Δ is the 3-dimensional scalar Laplacian, the algorithm becomes,

$$\Delta\bar{\phi}^{n+1} = N(\phi^n), \tag{54a}$$

$$\phi^{n+1} = \phi^n + \omega(\bar{\phi}^{n+1} - \phi^n). \tag{54b}$$

During the early stages of collapse, before a black hole forms, the value of this weight is largely unimportant and can be taken as unity. Once a black hole forms, the solutions for the conformal factor are in a very nonlinear regime and the use of a correct weight is crucial to finding a solution. The optimal weight appears to be $\omega = 0.22$ once a black hole forms and values $\omega > 0.5$ appear to be divergent.

An evolution equation for ϕ is obtained by combining equations (32) and (33) and this is used to provide a first approximation for the elliptic solver. Since such an equation exists, we

use it rather than extrapolate as was done for the lapse function α above. The boundary conditions for ψ on axis, equator, and origin are similar to those for the lapse and are straightforwardly applied. The Robin condition at the outer boundary (given in section 2) is enforced by

$$\psi_{jm+1/2} = [\psi_{jm-1/2}(1 - \frac{\Delta r_{jm}}{2r_{jm}}) + \frac{\Delta r_{jm}}{r_{jm}}] \ (1 + \frac{\Delta r_{jm}}{2r_{jm}})^{-1} \qquad (55)$$

It is important to note before going on what behavior the various vector and tensor components are near r=0 and θ=0, the singular points of the coordinate system. This is necessary both to understand the boundary conditions on axis and at the origin and to facilitate "regularization" of the differencing near these points. The latter point is most important in handling the vector and tensor elliptic systems. The local dependence of these variables is determined (Evans 1984b) by enforcing the symmetry assumptions and by assuming the local cartesian components are Taylor expandable about r=0 in cartesian coordinates. These series are then transformed back to spherical polar coordinates and written as an order expansion in powers of r.

Only the lowest order dependence will be given. The vector components β^r, β^θ have the form

$$\frac{\beta^r}{r} = c_0 + c_1 \sin^2\theta + O(r^2), \ \beta^\theta = c_1 \sin\theta \cos\theta + O(r^2) \qquad (56)$$

where c_0, c_1 are constants (note β^θ angular dependence determined locally by β^r/r). The behavior of W^i and V^i are of the same form. The momentum density is similar except given in covariant form:

$$S_r = r(c_2 + c_3 \sin^2\theta) + O(r^3), \ S_\theta = c_3 r^2 \sin\theta\cos\theta + O(r^4). \qquad (57)$$

The metric component $\ln T$ has the property

$$\ln T = c_4 r^2 \sin^2\theta \ [1 + O(r^2)]. \qquad (58)$$

The extrinsic curvature components are linked together locally by

$$\begin{aligned} \lambda &= 3c_5 \sin^2\theta \ [1 + O(r^2)], \\ K^\phi{}_\phi &= c_5 \ [1 + O(r^2)], \\ \frac{K^r{}_\theta}{r} &= 3c_5 \sin\theta\cos\theta \ [1 + O(r^2)]. \end{aligned} \qquad (59)$$

All other quantities behave as transformed scalars; they are analytic functions of the form $f(r^2\cos^2\theta, r^2\sin^2\theta)$, which satisfy the assumed symmetries.

The second order shift potential equations (30) and (31) are decoupled in the potentials χ and Φ. Furthermore the appearance of 2-dimensional Laplace operators allows these equations to be finite Fourier decomposed in the angular direction and replaced by a set of ordinary differential equations (ODEs). This avoids the use of iterative or relaxation solution methods, as was used for the lapse equation and the Hamiltonian constraint equation above, and significantly speeds the solution of these equations on the computer.

A finite Fourier transform of χ, Φ, and the source terms in (26) and (27):

$$P = \alpha\,(2K^{r}{}_{r} + K^{\phi}{}_{\phi}), \tag{60}$$

$$Q = 2\alpha\,\frac{K^{r}{}_{\theta}}{r}, \tag{61}$$

gives

$$\chi_{k+1/2} = a_0 + 2\sum_{m=1}^{km-3} a_m \cos 2m\theta_{k+1/2},$$

$$\Phi_k = 2\sum_{m=1}^{km-3} b_m \sin 2m\theta_k,$$

$$P_{k+1/2} = p_0 + 2\sum_{m=1}^{km-3} p_m \cos 2m\theta_{k+1/2},$$

$$Q_k = 2\sum_{m=1}^{km-3} q_m \sin 2m\theta_k. \tag{62}$$

These transforms are consistent with the parities of the functions under axisymmetry and equatorial plane symmetry. The inverse transforms are

$$p_m = \left(\frac{1}{km-2}\right)\sum_{k=2}^{km-1} P_{k+1/2} \cos 2m\theta_{k+1/2},$$

$$q_m = \left(\frac{1}{km-2}\right)\sum_{k=3}^{km-1} Q_k \sin 2m\theta_k, \tag{63}$$

with identical expressions for the amplitudes a_m and b_m. In the above expressions, the radial index is suppressed; all amplitudes are implicitly functions of r.

From the local dependence (56) for the shift vector near r = 0, it can be shown (Evans 1984b) that the definitions (28) and (29) for the potentials imply a singular local behavior in χ which shows up in a_0:

$$a_0 = \text{constant} \times \ln r, \tag{64}$$

near r = 0. Hence the amplitudes a_0 and p_0 are handled separately. The p_0 amplitude in (63) is just the angle average of P. So by defining

$$\left\langle \frac{\beta^r}{r} \right\rangle = \left(\frac{1}{km-2}\right) \sum_{k=2}^{km-1} \left(\frac{\beta^r}{r}\right)_{k+1/2}, \tag{65}$$

this part of the decomposition of the shift vector can be found by directly integrating (26):

$$\left\langle \frac{\beta^r}{r} \right\rangle = - \int_r^{r_m} p_0 \frac{dr}{r} + \left\langle \frac{\beta^r}{r} \right\rangle \Big|_{r=r_m}. \tag{66}$$

A discussion of the choice of boundary conditions for (66) is found in Evans (1984b). The amplitude a_0, containing the singular behavior of the potential χ, is never explicitly calculated.

With the transforms defined in (62) and (63), the decomposition of (30) and (31) becomes

$$r\partial_r(r\partial_r a_m) - 4m^2 a_m = p_m, \tag{67}$$

$$r\partial_r(r\partial_r b_m) - 4m^2 b_m = q_m. \tag{68}$$

These are a set of uncoupled ODEs for each m = 1, ..., km-3. With boundary values given at both r = 0 and $r = r_m$, they are solved using the tridiagonal algorithm (Roache, 1976). The inner boundary conditions are $\partial_r a_m = \partial_r b_m = 0$ at r = 0. Discussion of the physical conditions on the shift at large radius is beyond our purpose here and we refer instead to Evans (1984b).

Finally we close with a discussion of the numerical problems encountered with the accuracy of finite differencing coupled elliptic systems near the singular points of curvilinear coordinate systems and the techniques we have used to circumvent these numerical irregularities. We employ spherical coordinates in our calculations and hence problems in the finite difference approximation appear at the origin, r = 0, and to a lesser extent on the symmetry axis, $\theta = 0$. Similar numerical regularity problems also occurred in an earlier version of this code which employed topological cylindrical coordinates (Wilson, 1979). In that case the irregularities showed up along the entire (coordinate singular) symmetry axis. Similar numerical irregularities have long been a

source of problems in using 2-dimensional numerical relativity codes. We have developed techniques for eliminating this aberrant behavior in our spherical coordinate numerical relativity code. The general method however appears immediately applicable to other coordinate topologies. We have identified two causes of these numerical irregularities near symmetry points. The first is due to the loss of finite difference accuracy and increase of truncation errors near these regions in curvilinear coordinate systems. The second is related to the appearance of nontrivial, local homogeneous solutions to coupled elliptic systems.

The usual arguments on the formal size of truncation errors in finite difference approximations are based on the use of a Taylor expansion. For a problem in cartesian-like coordinates with zone increments Δx, centered spatial differences will produce truncation errors with respect to the corresponding derivatives they replace of order $(\Delta x/\ell)^2$, where ℓ is the characteristic physical length. These errors can be arbitrarily reduced with increase in the resolution (i.e. $\Delta x \to 0$). The problem with finite differencing in curvilinear coordinates, near the special points or regions of the coordinate system, is that Taylor series do not in general exist there. One encounters in spherical coordinates differential operators of the form $\frac{1}{r}\,\partial_r$, for example (similarly one has $\frac{1}{\rho}\,\partial_\rho$ in cylindrical coordinates). With the explicit appearance of the radial coordinate, attempts to produce centered finite differences of such operators will produce truncation errors that are the maximum of $(\Delta r/\ell)^2$ or $(\Delta r/r)^2$, where ℓ is again the characteristic physical length. Far from the origin of coordinates these errors can be made sufficiently small. However in the vicinity of $r = 0$, the errors associated with most finite difference representations will be of order unity (or worse).

We can illustrate this problem and its solution with a specific example. Consider the radial second order operator of the flat space 3-dimensional Laplacian:

$$\frac{1}{r^2}\,\partial_r(r^2\partial_r\phi). \tag{69}$$

Let us consider that this operator produces zone centered values, i.e. located at positions $r_{j+1/2}$ and that ϕ is zone centered as well: $\phi_{j+1/2}$. Using our mesh definitions, one can straightforwardly difference (69):

$$\frac{1}{r^2_{j+1/2}} \frac{1}{\Delta r_{j+1/2}} [r^2_{j+1} \frac{1}{\Delta r_{j+1}} (\psi_{j+3/2} - \psi_{j+1/2})$$

$$- r^2_j \frac{1}{\Delta r_j} (\psi_{j+1/2} - \psi_{j-1/2})]. \tag{70}$$

Let us assume further that we can expect ψ to have the local radial dependence

$$\psi(r) = c_0 + c_1 r^2 + 0(r^4), \tag{71}$$

i.e. like the gravitational potential or our conformal factor. Application of (69) on this ψ gives locally the analytic value $6c_1$. If however we take $\psi_{j+1/2} = c_0 + c_1 r^2_{j+1/2}$ and use (70) we obtain

$$c_1 \frac{1}{r^2_{j+1/2}} \frac{1}{\Delta r_{j+1/2}} [r^2_{j+1} (r_{j+3/2} + r_{j+1/2})$$

$$- r^2_j (r_{j+1/2} + r_{j-1/2})]. \tag{72}$$

Evaluating this at the first three radial locations, $j = 2, 3, 4$, yields the values $8.0\ c_1$, $6.22\ c_1$, $6.08\ c_1$, respectively. Hence, it can be seen that the errors near the origin in such a straightforward finite differencing (70) of (69) are of order unity.

The solutions to these problems is to choose the specific finite difference representation for the operator in question which reproduces the expected analytic result under the assumption that the general local dependence of the function is known. This altered finite difference operator for (69) for example will differ from the straightforward one (70) away from the origin only at the level of second order, which is already conceded to the approximation as a whole. For (69), we would use instead

$$\frac{3}{r^3_{j+1} - r^3_j} [\frac{2r^3_{j+1}}{r_{j+3/2} + r_{j+1/2}} \frac{1}{\Delta r_{j+1}} (\psi_{j+3/2} - \psi_{j+1/2})$$

$$- \frac{2r^3_j}{r_{j+1/2} + r_{j-1/2}} \frac{1}{\Delta r_j} (\psi_{j+1/2} - \psi_{j-1/2})], \tag{73}$$

which, assuming (71) as the expected form for ψ, reproduces the analytic value.

A second problem which will be typically encountered in solving coupled elliptic systems is local homogeneous solutions. We can illustrate why this is not normally a problem by considering the scalar Poisson equation

$$\Delta\phi = 4\pi\rho. \tag{74}$$

The homogeneous solution for this equation is just a constant, say c_0. Assuming our symmetry conditions, the local dependence of ϕ near $r = 0$ would be $\phi = c_0 + r^2(c_1 + c_2 \sin^2\theta) + \theta(r^4)$, in spherical coordinates. Regardless of whether this equation (74) is written in cartesian coordinates or spherical coordinates prior to finite differencing, the difference representations of the partial derivatives in the Laplacian will identically cancel off the constant c_0. The finite differencing of (74) can then concentrate on reproducing the expected next order behavior in ϕ. The value c_0 is of course only determined by the global solution of (74) once suitable boundary values have been prescribed.

The situation changes drastically when one considers vector or tensor (or in general multi-component coupled) elliptic systems. Consider a 2-tensor K^i_j which exhibits our assumed symmetries including a tracefree condition (i.e. like the extrinsic curvature tensor). The cartesian components in the limit $r \to 0$ (Evans, 1984b) have the form

$$\lim_{r\to 0} K^i_j = \text{diag}\,[c_5,\ c_5,\ -2c_5], \tag{75}$$

where c_5 is a constant. If a tensor-like Laplace operator, like the "tensor Laplacian" (43), in cartesian coordinates operates on (75), this "constant" or homogeneous solution will be annihilated. The same is true of a finite difference representation. However, if the tensor (75) is transformed to spherical coordinates, this local homogeneous solution will be of the form (59) which has angular dependence! If the finite difference operator is to produce accurate results, these terms must still be identically annihilated. Figure 1 shows the irregular behavior near $r = 0$ produced in the component $K^\phi{}_\phi$ when no attention is paid to these details. An anomalous numerical "spike" occurs in the first five to ten radial zones. The solution to the problems arising from local homogeneous solutions is to rewrite the differential equations in a form which allows the difference equations to cancel off these terms. This is the reason for writing equations (37), (38) and (44), (45) in the form given in this paper. The reader can verify that the underlined terms in these equations allow the expected local dependence of W^i, (56), and K^i_j, (59), to drop through. Once both of these numerical techniques are applied, the local behavior of the solutions near $r = 0$ is greatly improved. This can be seen in Figure 2 which shows the effect of these

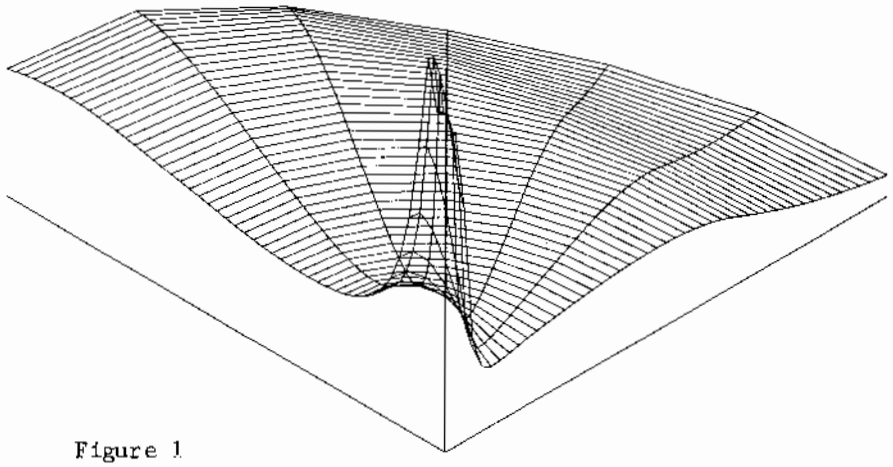


Figure 1

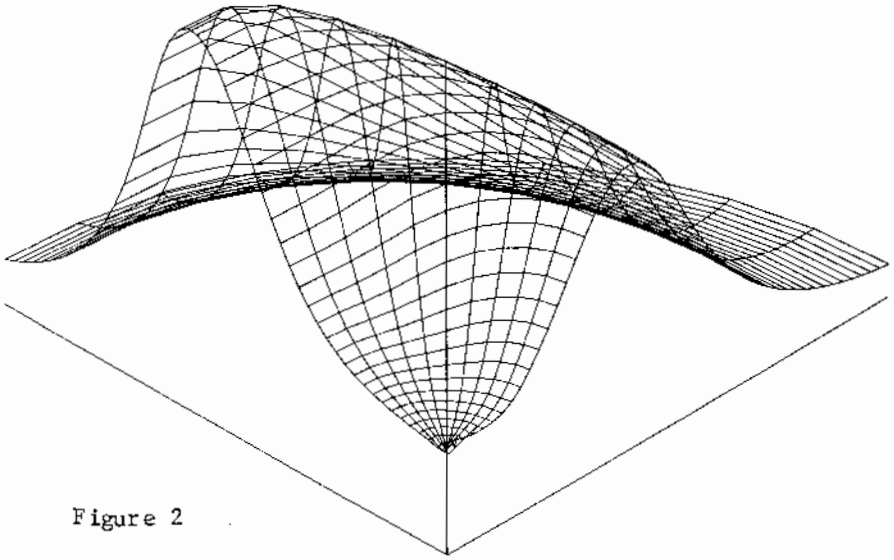


Figure 2

Figure 1. The local behavior near r = 0 in the extrinsic curvature component $K^{\phi}{}_{\phi}$. An anomalous numerical "spike" is evident at the origin affecting the first 5-10 zones. In this figure, the symmetry axis is to the right and the equatorial plane to the left.

Figure 2. The same component plotted after the finite differencing has been "regularized." Note that the vertical scales in the two figures are different, with Figure 1 being dominated by the numerical error. Hence, there is considerable improvement in Figure 2.

changes on the same component plotted in Figure 1. More details of these techniques can be found in Evans (1984b).

4. CONCLUSION

We have presented a general approach for solving the Einstein equations of general relativity coupled to hydrodynamics. This coupled nonlinear system of partial differential equations naturally split into equations of constraint and of evolution. The constraints can be solved for the longitudinal pieces of the gravitational field which generalizes the Newtonian scalar potential. The evolution equations determine the generation and propogation of gravitational radiation, a feature not found in Newtonian gravity. For relativistic systems, such as supernova core collapse, this full approach is the only reliable calculational tool available.

The general framework is then specialized to the axisymmetric case in which no rotation occurs. In addition, the spacetime is assumed to be asymptotically flat. A particular choice of coordinates simplifies the differential equations considerably. A computer code was written using finite difference techniques to solve these equations. Some crucial details are spelled out which are unique to differencing the Einstein equations.

Although space does not allow us to give examples of the use of this code, it is a working production code. Some runs simulating highly oblate collapse to post-nuclear densities are discussed in Evans (1984a,b). These runs are the first to be able to calculate the gravitational radiation emitted in highly nonspherical relativistic collapse. Other studies to elucidate the physics of strong dynamic gravitational fields are currently underway.

The approach we use will be extended to include rotation. This will yield an alternate technique to those used by Nakamura, et al. (1980) or Bardeen and Piran (1983). Going beyond that one has good near-term prospects to use our approach to study full four dimensional spacetimes (three space + time). This can be done in either the asymptotically flat or the cosmological regime. This final step in studying gravitational physics will require the new generation of supercomputers with multiprocessors and large memories. In addition, more efficient numerical algorithms to solve the Einstein equations will be developed. A more detailed and realistic treatment of other microphysics will also be added. We believe this will create a rich new field of physics: computational relativity.

ACKNOWLEDGEMENTS

We have benefited from discussions with Joan Centrella, Pieter Dykema, Richard Isaacson, James LeBlanc, Richard Matzner, Michael Norman, Karl-Heinz Winkler, and James W. York, Jr. We wish to thank the Max-Planck-Institüt für Physik und Astrophysik, Institüt für Astrophysik for their hospitality. Much of this research was conducted at the Lawrence Livermore National Laboratory and the Center for Relativity, University of Texas at Austin. Financial support was partially provided by the Associated Western Universities Graduate Fellowship Program, the National Science Foundation under grant number PHY 83-08826, and the Department of Energy contract number W-7405-ENG-48.

BIBLIOGRAPHY

Arnowitt, R., S. Deser, and C.W. Misner: 1962, "The Dynamics of General Relativity," in Witten (ed.), Gravitation: An Introduction to Current Research, John Wiley, New York, pp. 227-265.

Bardeen, J.M. and T. Piran: 1983, "General Relativistic Axisymmetric Rotating Systems: Coordinates and Equations," Phys. Reports **96**, pp. 206-250.

Brill, D.R.: 1959, "On the Positive Definite Mass of the Bondi-Weber-Wheeler Time-Symmetric Gravitational Waves," Ann. Phys. **7**, pp. 466-483.

Cantor, M.: 1979, "A Necessary and Sufficient Conditon for York Data to Specify and Asymptotically Flat Spacetime," J. Math. Phys. **20**, pp. 1741-1744.

Centrella, J. and J.R. Wilson: 1983, "Planar Numerical Cosmology I. The Differential Equations," Astrophys. J. **273**, pp. 428-435.

Centrella, J. and J.R. Wilson: 1984, "Planar Cosmology II. The Difference Equations and Numerical Tests," Astrophys. J. Suppl. **54**, pp. 229-250.

Dykema, P.G.: 1980, "Numerical Simulation of Axisymmetric Gravitational Collapse," Ph. D. thesis, Univ. of Texas at Austin (unpublished).

Eardley, D. and L. Smarr: 1979, "Time Functions in Numerical Relativity: Marginally Bound Dust Collapse," Phys Rev. **D19**, pp. 2239-2259.

Eardley, D.: 1979, "Global Problems in General Relativity," in L. Smarr (ed.), Sources of Gravitational Radiation, Cambridge University Press, Cambridge, pp. 127-138.

Eppley, K.: 1979, "Pure Gravitational Waves," in L. Smarr (ed.), Sources of Gravitational Radiation, Cambridge University Press, Cambridge, pp. 275-292.

Estabrook, F., H. Wahlquist, S. Christensen, B. DeWitt, L. Smarr, and E. Tsiang: 1973, "Maximally Slicing a Black Hole," Phys. Rev. **D7**, pp. 2814-2817.

Evans, C.R.: 1984a, "A Method for Numerical Simulation of Gravitational Collapse and Gravitational Radiation Generation," in J. Centrella, R. Bowers, J. LeBlanc, and M. Le Blanc (eds.), Numerical Astrophysics: A Meeting in Honor of James Wilson, Jones and Bartlet, Portola Valley CA, (in press).

Evans, C.R.: 1984b, "A Method for Numerical Relativity: Simulation of Axisymmetric Gravitational Collapse and Gravitational Radiation Generation," Ph. D. thesis, University of Texas at Austin (unpublished).

Haugan, M.P., S.L. Shapiro, and I. Wasserman: 1982, "The Suppression of Gravitational Radiation from Finite-Size Stars Falling Into Black Holes," Astrophys. J. **257**, pp. 283-290.

Hawley, J.F., L.L. Smarr, and J.R. Wilson: 1984, "A Numerical Study of Nonspherical Black Hole Accretion. II. Finite Differencing and Code Calibration," Astrophys. J. Suppl. **55**, pp. 211-246.

Landau, L.D. and E.M. Lifshitz: 1941, Teoriya Polya, Nauka, Moscow, (English translation The Classical Theory of Fields), Addison-Wesley, Cambridge.

Leith, C.E.: 1965, "Numerical Simulation of the Earth's Atmosphere," Methods of Computational Physics, **4**, pp. 1.

Lichnerowicz, A.: 1944, "L'integration des Equations de la Gravitation Relativiste et le Probleme des n Corps," J. Math. Pure Appl. **23**, pp. 37-63.

May, M. and R.H. White: 1966, "Stellar Dynamics and Gravitational Collapse," in B. Alder, S. Fernbach, and M. Rotenberg (eds.), Methods in Computational Physics, Vol. 7, Academic Press, New York, pp. 219-258.

Misner, C.W. and D.H. Sharp: "Relativistic Equations for Adiabatic, Spherically Symmetric Gravitational Collapse," Phys. Rev. **136**, pp. B571-B577.

Müller, E. and W. Hillebrandt: 1981, "The Collapse of Rotating Stellar Cores," Astron. Astrophys. **103**, pp. 358-366.

Müller, E.: 1982, "Gravitational Radiation From Collapsing Rotating Stellar Cores," Astron. Astrophys. **114**, pp. 53-59.

Nakamura, T., K. Maeda, S. Miyama and M. Saski: 1980, "General Relativistic Collapse of an Axially Symmetric Star. I. The Formulation and The Initial Data," Prog. Theor. Phys. **63**, pp. 1229-1244.

Nakamura, T. and M. Saski: 1981, "Is Collapse of a Deformed Star Always Effectual for Gravitational Radiation," Phys. Lett. **106**, pp. 69-72.

Nakamura, T.: 1981, "General Relativistic Collapse of Axially Symmetric Stars Leading to the Formation of Rotating Black Holes," Prog. Theor. Phys. **65**, pp. 1876-1890.

O'Murchadha, N. and J.W. York: 1974, "Initial-Value Problem of General Relativity. I. General Formulation and Physical Interpretation," Phys. Rev. **D10**, pp. 428-436.

Piran, T.: 1980, "Numerical Codes for Cylindrical General Relativistic Systems," J. Comp. Phys. **35**, pp. 254-283.

Piran, T.: 1983, "Methods of Numerical Relativity," in N. Deruelle and T. Piran (eds.), Gravitational Radiation, North Holland, Amsterdam, 203.

Roache, R.J.: 1976, Computational Fluid Dynamics, Hermosa Publishers, Albuquerque.

Shapiro, S.L. and S.A. Teukolsky: 1979, "Gravitational Collapse of Supermassive Stars to Black Holes: Numerical Solution of the Einstein Equations," Astrophys. J. Lett. **234**, pp. L177-L181.

Shapiro, S.L. and S.A. Teukolsky: 1980, "Gravitational Collapse to Neutron Stars and Black Holes: Computer Generation of Spherical Spacetimes," Astrophys. J. **235**, pp. 199-215.

Smarr, L.L.: 1975, "The Structure of General Relativity with a Numerical Illustration: The Collision of Two Black Holes," Ph.D. Dissertation, The University of Texas at Austin, (unpublished).

Smarr, L.L.: 1977, "Spacetimes Generated by Computers: Black Holes with Gravitational Radiation," Ann. N.Y. Acad. Sci. **302**, pp.569-604.

Smarr, L.: 1979, "Gauge Conditions, Radiation Formulae and the Two Black Hole Collision," in L. Smarr (ed.) Sources of Gravitational Radiation, Cambridge University Press, Cambridge, pp. 245-274.

Smarr, L.L.: 1984, "Computational Relativity: Numerical and Algebraic Approaches," to appear in the Proceedings of the Tenth International Conference on General Relativity and Gravitation.

Smarr, L.L., C. Taubes, and J.R. Wilson: 1980, "General Relativistic Hydrodynamics: The Comoving, Eulerian, and Velocity Potential Formalisms," in F. Tipler (ed.) Essays in General Relativity: A Festschrift for A. Taub, New York, Academic Press, pp. 157-183.

Smarr, L. and J.W. York: 1978a, "Radiation Gauge in General Relativity," Phys. Rev. **D17**, pp. 1945-1956.

Smarr, L. and J.W. York: 1978b, "Kinematical Conditions in the Construction of Spacetime," Phys. Rev. **D17**, pp. 2529-2551.

Thorne, K.S.: 1980a, "Gravitational-Wave Research: Current Status and Future Prospects," Rev. Mod. Phys. **52**, pp. 285-297.

Thorne, K.S.: 1980b, "Multipole Expansions of Gravitational Radiation," Rev. Mod. Phys. **52**, pp. 299-339.

Wheeler, J.A.: 1964, "Geometrodynamics and the Issue of the Final State," in C. DeWitt and B.S. DeWitt (eds.), Relativity, Groups, and Topology, Gordon & Breach, New York, pp. 317-522.

Wilson, J.R.: 1977, "A Numerical Study of Rotating Relativistic Stars," in R. Giaconni and R. Ruffini (eds.), Proceedings of the International School of Physics Enrico Fermi LXV, Amsterdam, N. Holland, pp.644-675.

Wilson, J.R.: 1979, "A Numerical Method for Relativistic Hydrodynamics," in L. Smarr (ed.), Sources of Gravitational Radiation, Cambridge University Press, Cambridge, pp. 423-446.

York, J.W.: 1971, "Gravitational Degrees of Freedom and the Initial-Value Problem," Phys. Rev. Lett. **26**, pp. 1656-1658.

York, J.W.: 1972, "Role of the Conformal Three-Geometry in the Dynamics of Gravitation," Phys. Rev. Lett. **28**, pp. 1082-1085.

York, J.W.: 1973, "Conformally Invariant Orthogonal Decomposition of Symmetric Tensors on Riemannian Manifolds and the Initial-Value Problem of General Relativity," J. Math. Phys. **14**, pp. 456-464.

York, J.W.: 1979, "Kinematics and Dynamics of General Relativity," in L. Smarr (ed.), Sources in Gravitational Radiation, Cambridge University Press, Cambridge, pp. 83-126.

York, J.W. and T. Piran: 1982, "The Initial Value Problem and Beyond," in R. Matzner and L. Shepley (eds.), Spacetime and Geometry, University of Texas Press, Austin, pp. 147.